Vol 16 No 7, July 2007
1009-1963/2007/16(07)/2142-06
Chinese Physics
© 2007 Chin. Phys. Soc.
and IOP Publishing Ltd

Research on CeO_2 cap layer for YBCO-coated conductor*

Shi Dong-Qi(石东奇)[a], Ma Ping(马 平)[b]†, Ko Rock-Kil[c], Kim Ho-Sup[c], Chung Jun-Ki[c], Song Kyu-Jeong[c], and Park Chan[d]

[a] *Institute for Superconducting and Electronic Materials, University of Wollongong, Australia*
[b] *State Key Laboratory for Artificial Microstructure and Mesoscopic Physics, School of Physics, Peking University, Beijing* 100871, *China*
[c] *Korea Electrotechnology Research Institute, Changwon, Kyungnam, Korea*
[d] *School of Materials Science & Engineering, College of Engineering, Seoul National University, Seoul 151-744, Korea*

(Received 10 October 2006; revised manuscript received 31 January 2007)

Two groups of coated conductor samples with different thicknesses of CeO_2 cap layers deposited by pulsed laser deposition (PLD) under the same conditions have been studied. Of them, one group is of CeO_2 films, which are deposited on stainless steel (SS) tapes coated by IBAD-YSZ (IBAD-YSZ/SS), and the other group is of CeO_2/YSZ/Y_2O_3 multilayers, which are deposited on NiW substrates by PLD for the fabrication of YBCO-coated conductor through the RABiTS approach. YBCO film is then deposited on the tops of both types of buffer layers by PLD. The effects of the thickness of the CeO_2 film on the texture of the CeO_2 film and the critical current density (J_c) of the YBCO film are analysed. For the case of CeO_2 film on IBAD-YSZ/SS, there appears a self-epitaxy effect with increasing thickness of the CeO_2 film. For CeO_2/YSZ/Y_2O_3/NiW, in which the buffer layers are deposited by PLD, there occurs no self-epitaxy effect, and the optimal thickness of CeO_2 is about 50 nm. The surface morphologies of the two groups of samples are examined by SEM.

Keywords: coated conductor, buffer layer, self-epitaxy, CeO_2
PACC: 8115, 7470V, 7475

1. Introduction

Two main methods have been developed for the fabrication of YBCO-coated conductors: one is through an ion-beam-assisted-deposition (IBAD) process,[1,2] the other is by a rolling-assisted biaxially textured substrate (RABiTS) approach.[3,4] Currently, a CeO_2 buffer layer plays an important role in both processes.

CeO_2 film was first used as a buffer layer on a single crystal $LaAlO_3$ for YBCO in 1991.[5] It has been demonstrated that a CeO_2 film is chemically and structurally compatible with superconducting YBCO film.[6] In 1996 Goyal *et al*[7] reported for the first time on a high critical current density (0.9 MA/cm^2) YBCO film deposited on Ni substrates with a CeO_2 and yttrium-stabilized zirconia (YSZ, 10 atm%Y) buffer layer through RABiTS. Since then, CeO_2 films have been widely used as buffer layers with various single crystalline and metallic substrates.[8] The standard architectures established now are CeO_2/YSZ/CeO_2/Ni-alloy or CeO_2/YSZ/Y_2O_3/Ni-alloy for the RABiTS approach, and CeO_2/IBAD-YSZ or CeO_2/IBAD-$Gd_2Zr_2O_7$ on no-texture metal tape for the IBAD approach. With these architectures, the CeO_2 cap layer provides good lattice matching for the subsequent YBCO layer.[9] For the RABiTS approach, the CeO_2 cap layer on YSZ also provides chemical compatibility by suppressing the growth of $BaZrO_3$ which may occur at a YSZ/YBCO interface and cause the degradation of the critical current in the YBCO layer.[10] So the thickness of CeO_2 film should be sufficient to obstruct this reaction. However, it was reported that an epitaxial CeO_2 layer cracked extensively when its thickness exceeded several tens of nanometres on Ni or YSZ film.[11,12]

For the IBAD approach, recently, the SRL-Nagoya Coated Conductor Centre (NCCC)[13−15] has used the IBAD and the PLD methods to fabricate the

*Project supported by the 21st Century Frontier R&D Program of the Center for Applied Superconductivity Technology, funded by the Ministry of Science and Technology, Republic of Korea.
†Corresponding author. E-mail: maping@pku.edu.cn

buffer layers each with a CeO_2 layer as a cap layer serving for a coated conductor. It was found that the CeO_2 film deposited on the IBAD seed layer by PLD effectively increased the in-plane alignment with the thickness of the CeO_2 buffer layer increasing. The IBAD seed layer can be of YSZ or $Gd_2Zr_2O_7$ (GZO). This effect is called 'self-epitaxy' in the sense that no assistance is needed; such is provided by the Ar ions in the IBAD method. This new phenomenon results in small misorientation angles among grains, thus leading to a reduction in the weak-link induced degradation of J_c in the grain boundaries of the conductor.

In summary, the thickness of a CeO_2 capping layer is an important factor for the quality of coated conductors, and an optimal thickness should be ascertained, especially for the RABiTS approach. The present work investigates the effects of the thickness of a PLD-deposited CeO_2 film on the in-plane texture and the J_c of YBCO-coated conductor for both IBAD and RABiTS samples. The main emphasis of this work is placed on a comparison between the CeO_2 films deposited separately on the RABiTS and IBAD substrates under the same conditions.

2. Experiment

In the PLD system, stoichiometric Y_2O_3, YSZ, CeO_2, and YBCO ceramic targets (2 inches (50.8 mm) in diameter) were ablated by an excimer KrF pulsed laser (LPX220i with a wavelength of 248 nm from Lambda Physik). Biaxially textured Ni–3at%W substrates with a size of $3 \times 10\,mm^2$ were attached with silver paste to the target holder (also the heater) which directly faced the target. The deposition temperature was measured by a thermocouple located in the heater block.

The particulars of the deposition system were as follows: a laser beam being incident upon the target at an angle of 60° with respect to the normal of the target; target-substrate distance being 65 mm; target rotation rate 25rpm; background pressure 1.33×10^{-4} Pa. The deposition was carried out by using a laser with a repetition rate of 3–20 Hz, and a laser spot of $5 \times 1\,mm^2$ and a pulsed laser energy density of 2–3J/cm^2 on the target.

The D8 DISCOVER x-ray diffraction system with general area detector diffraction solution (GADDS) from Bruker was used to analyse the orientation of films. In this system the x-ray wavelength is 0.1541837 nm. In the XRD (x-ray diffraction) examination, $\theta \sim 2\theta$ scans, ω-scans and ϕ-scans were performed with sample oscillation using a 1/4-circle Eulerian cradle xyz stage. A scanning electron microscope (SEM) was used to investigate the surface morphology, microstructure, and defects in the YBCO films.

3. Results and characterization

An IBAD template (IBAD-YSZ/SS) manufactured in Germany was used. A full width at half maximum (FWHM) of the ϕ-scan ($\Delta\phi$) of the YSZ was about 10.4°, and the thickness of the YSZ was about 1 μm. Ni-3at%W tapes (NiW) with a biaxial texture, manufactured through a standard cold rolling and recrystallization process, were provided by Oxford Superconducting Technology. The in-plane and out-of-plane textures of the NiW substrates used in this work were evaluated from the FWHM of the ϕ-scan ($\Delta\phi$) and the ω-scan ($\Delta\omega$), respectively. The NiW substrates possess a sharp biaxial texture with in-plane and out-of-plane textures of $\Delta\phi$ =7–9° and $\Delta\omega$ =7–8°.

Two groups of samples with different thicknesses of CeO_2 capping layers deposited by PLD were studied. Figure 1 gives the schematic diagrams of the two groups of samples.

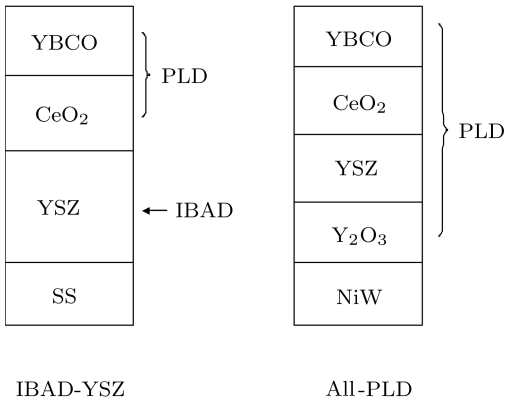


Fig.1. Schematic diagrams of the two groups of samples.

3.1. IBAD-YSZ samples

Firstly, CeO_2 films with different thicknesses from 25 nm to 800 nm were deposited on CeO_2/IBAD-YSZ/SS by PLD, with the results called IBAD-YSZ samples from now on. The deposition was carried out at an ambient temperature of 700–780 °C in

1.33×10^{-2}–1.33×10^{-1}Pa O_2 with a laser energy of 200 mJ/pulse and repetition rate of 10 Hz. The XRD ϕ-scans were used to examine the orientation of the CeO_2 films. The FWHM value of the XRD ϕ-scan for the (111) plane gradually decreased as the CeO_2 film thickness increased from 25 nm to 800 nm, indicating that there was an effect of increasing in-plane alignment with increasing the thickness of the CeO_2 buffer layer. During the YBCO deposition, the heater temperature was in a range of 760–780 °C and the oxygen pressure in the chamber was 26.6 Pa. The laser repetition rate was at 10 Hz, and the laser energy density on the target was about 3J/cm^2. Immediately after being deposited, the YBCO film was quickly cooled to 550°C under the deposition pressure, and then held for 20 min under an oxygen pressure of 6.65×10^4 Pa. The thickness of the YBCO films was about 250nm. The T_{c0} of the YBCO films on the IBAD-YSZ samples was about 86–89 K and the J_c increased with increasing the in-plane alignment of the CeO_2, which resulted from the increasing of CeO_2 thickness (see Fig.2). This clearly confirmed that there was a 'self-epitaxy' effect in the CeO_2 films under these deposition conditions.

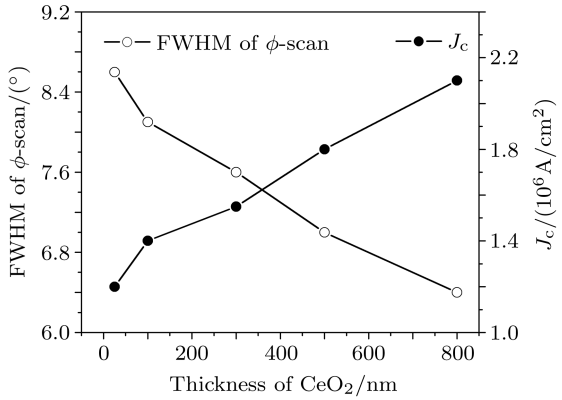


Fig.2. The relationships between the ϕ-scan FWHM and the thickness of the CeO_2 film and between the critical current density and the thickness of CeO_2 film, with the CeO_2 capping layers deposited on CeO_2/IBAD-YSZ/SS.

3.2. All-PLD samples

Another group of CeO_2/YSZ/Y_2O_3/NiW samples was prepared by using the RABiTS approach. During its heating, the substrate was prevented from oxidizing by introducing a 26.6 Pa Ar+4%H_2 reducing gas flow. The three buffer layers of CeO_2, YSZ and Y_2O_3 were prepared sequentially by PLD without breaking the vacuum.

The first Y_2O_3 layers were deposited on the NiW substrates at an ambient temperature of 650 °C, in a 26.6 Pa Ar+4%H_2 forming gas with a laser energy of 200 mJ/pulse and repetition rate of 10 Hz till their thickness reaching up to 150 nm. The YSZ with a thickness of 250 nm was deposited at 650–780 °C in 1.33×10^{-2} Pa O_2 with a laser energy of 200 mJ/pulse and repetition rate of 20 Hz. And then the CeO_2 layer was deposited as a capping layer at the same temperature as that of the YSZ in 1.33×10^{-2}–1.33×10^{-1} Pa O_2 with a laser energy of 200 mJ/pulse and repetition rate of 10 Hz. The CeO_2 thicknesses in the series of samples were 25 nm, 50 nm, 100 nm, 200 nm, 400 nm and 800 nm separately. The deposition rate of CeO_2 was about 35 nm/min.

The XRD θ–2θ scans for this group of RABiTS samples show that there exist only (00l) peaks for Y_2O_3, YSZ and the CeO_2 films, which means that the films have a pure c-axis orientation (Fig.3). YBCO films were prepared on the top of the CeO_2 under the same conditions as those for the IBAD-PLD samples above. Figure 4 shows the XRD ϕ-scans of a typical YBCO/CeO_2(400 nm)/YSZ/Y_2O_3/NiW sample. The J_c of this sample was about 1.2MA/cm^2 at 77 K and self-field. Figure 5 shows the T_c and I_c plots of this sample.

For this group of samples, the FWHM value of the XRD ϕ-scan for the (111) plane of CeO_2 did not change much with increasing CeO_2 film thickness, and the average value was about 8.2°, indicating that the in-plane alignment was not improved by increasing the thickness of the CeO_2 buffer layer. In other words, there was no self-epitaxy effect for the samples prepared using the RABiTS approach within this thickness range of CeO_2 film.

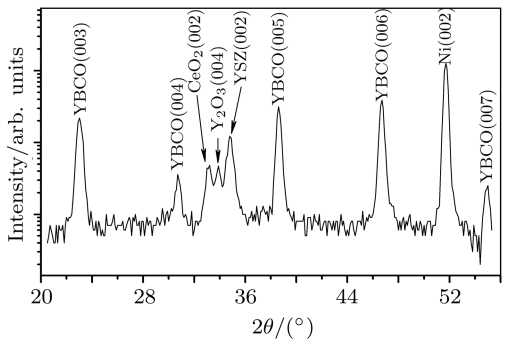


Fig.3. XRD θ–2θ scan for a YBCO/CeO_2 /YSZ/Y_2O_3/NiW sample in which all films were deposited by PLD.

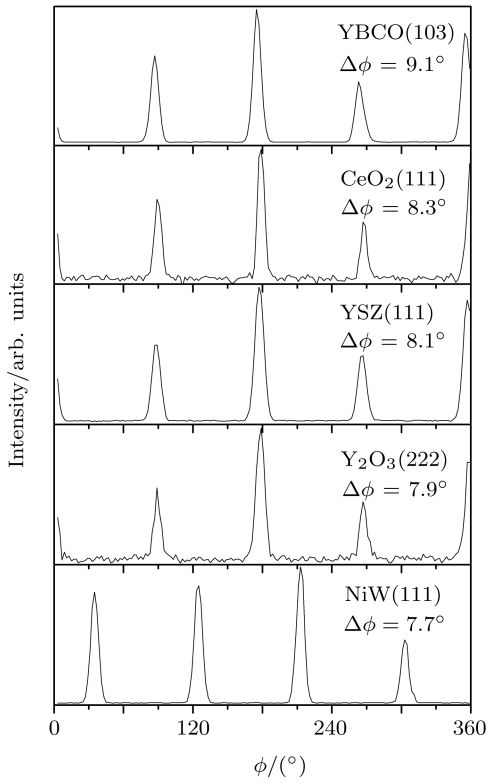


Fig.4. XRD ϕ-scans for a typical YBCO/CeO_2 (400 nm)/YSZ/Y_2O_3/NiW sample.

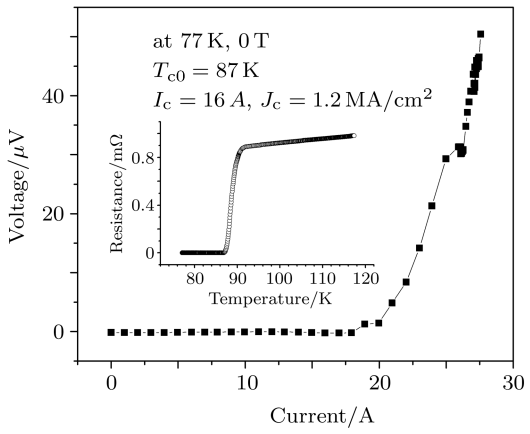


Fig.5. *I–V* curve and *R–T* curve for the same YBCO/CeO_2(400 nm)/YSZ/Y_2O_3/NiW sample.

Furthermore, the J_c of the YBCO film decreased with increasing the thickness of CeO_2 when the thickness was greater than 50 nm. Figure 6 shows the relationships between the FWHM of the ϕ-scan and the thickness of CeO_2 film, and between the critical current density and the thickness of CeO_2 film.

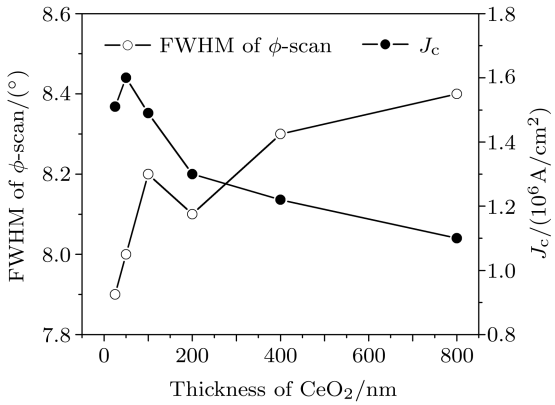


Fig.6. The relationships between the FWHM of the ϕ-scan and the thickness of CeO_2 film and between the critical current density for All-PLD (RABiTS) samples and the thickness of CeO_2 film.

3.3. Discussion

Figure 7 shows the surface of the CeO_2 layer on an IBAD-YSZ sample.

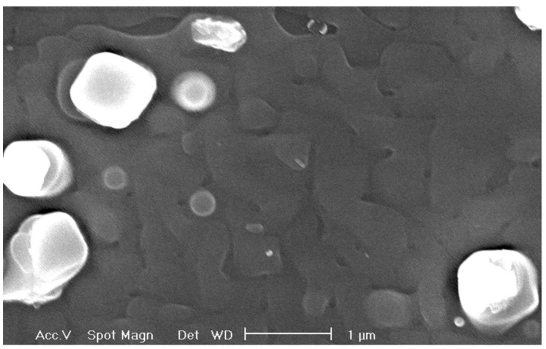


Fig.7. SEM image of the surface of the CeO_2 (800 nm)/IBAD-YSZ/SS sample.

Cracks in the CeO_2 film are frequently observed in RABiTS-based coated conductor samples when such a film is used as a seed layer on a Ni alloy tape, even when the CeO_2 layer is barely thicker than several tens of nanometres. In our work, it has been observed that there are no cracks in the CeO_2 layer on the IBAD tape until the CeO_2 layer reaches 800 nm in thickness. Yamada *et al*[13] have reported in their study that the first CeO_2 layer with 100 nm in thickness has grains with a few tens of nanometres in size, which is inherited from the IBAD seed layer, and when the CeO_2 film is thicker than 100 nm, the grains grow larger, up to 2 μm in diameter. In our SEM analysis, we have not observed such large grains. The average grain size is about 0.8 μm. This difference may arise from the

deposition rate, which is much lower in our deposition (35 nm/min) than in Yamada *et al*'s (100 nm/min). Even so, the grain size is still much larger than that in the thin CeO_2 film (about 0.1 μm), which shows that there appeared an abnormal growth of CeO_2 film. This feature is also consistent with the self-epitaxy effect.[15]

Figure 8 shows the surfaces of CeO_2 layers on the All-PLD samples. The CeO_2 film in Fig.8(a) is 100 nm thick, and it can be seen that the surface has some cracks, but is still relatively smooth. Figure 8(b) shows the surface of a CeO_2 layer with a thickness of 800 nm. From this image it can be seen that the surface of the CeO_2 layer is not only very rough, but also of layered structure. It is revealed that this is the reason why J_c degrades as the thickness of CeO_2 increases. Because the mismatch in thermal expansion coefficient between CeO_2 and Ni (∼29%) is much larger than between CeO_2 and YSZ (below 10%), we have observed that the CeO_2 as a cap layer on YSZ does not crack so seriously as the CeO_2 as a seed layer on Ni with the same thickness. The stress and strain in a CeO_2 layer increase with thickness increasing. The thicker the CeO_2 film on YSZ, the more cracks it has and the more rough its surface is. There has to be a compromise in the thickness of the CeO_2 cap layer between remaining crack-free and preventing the reaction between YSZ and YBCO. In this work, we have found an optimal thickness of CeO_2 on All-PLDs sample to be 50 nm.

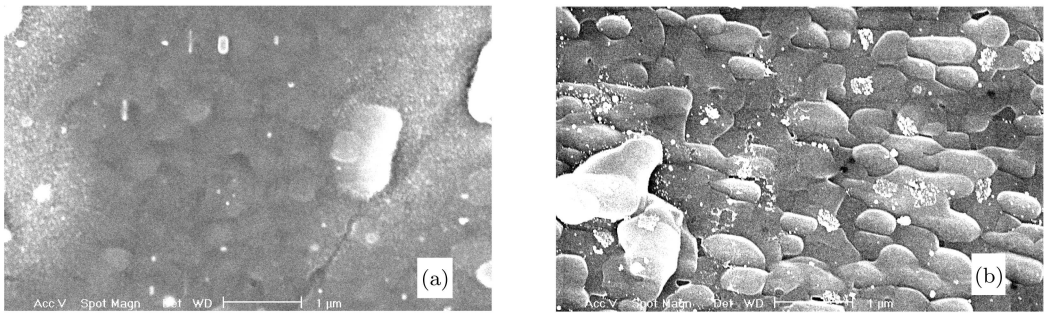


Fig.8. SEM images of the surfaces of $CeO_2/YSZ/Y_2O_3/NiW$ samples, with the thickness of CeO_2 layers being (a) 100 nm (b) 800 nm.

4. Summary

In this work, CeO_2 cap layers with different thicknesses have been deposited on the tops of CeO_2/IBAD-YSZ/SS by PLD, and the in-plane texture of the CeO_2 cap layer is improved with its thickness increasing. There are no cracks in the CeO_2 layer on the IBAD tape up to 800 nm in thickness, and the grain size of the CeO_2 is about 0.8 μm, which means that there appears an abnormal growth. This kind of CeO_2 film has a feature consistent with the self-epitaxy effect. In another group of $YBCO/CeO_2/YSZ/Y_2O_3/NiW$ samples, all buffer layers are deposited by PLD through the RABiTS approach. From the established relationships between the texture of CeO_2 film and the thickness of CeO_2 film and between the critical current density (J_c) of the YBCO film and the thickness of CeO_2 film, it can be seen that there occurs no self-epitaxy effect. The optimal thickness of the CeO_2 capping layer for the RABiTS approach is found to be about 50 nm. The J_c of the YBCO film deteriorates when the thickness of CeO_2 layer exceeds 50 nm. The reason why the J_c decreases is that the surface morphology becomes worse as the thickness of the CeO_2 increases.

References

[1] Kakimoto K, Iijima Y and Saitoh T 2000 *Physica* C **392–396** 783

[2] Wu X D, Foltyn S R, Arendt P, Townsend J, Adams C, Campbell I H, Tiwari P, Coulter Y and Peterson D E 1994 *Appl. Phys. Lett.* **65** 1961

[3] Norton D P, Goyal A, Budai J D, Christen D K, Kroeger D M, Specht E D, He Q, Saffian B, Paranthaman M, Klabunde C E, Lee D F, Sales B C and List F A 1996 *Science* **274** 755

[4] Goyal A, Norton D P, Budai J D, Paranthaman M, Specht E D, Kroeger D M, Christen D K, He Q, Saffian B, List F A, Lee D F, Martin P M, Klabunde C E, Hartfield E and

Sikka V K 1996 *Appl. Phys. Lett.* **69** 1795

[5] Wu X D, Dye R C, Muenchausen R E, Foltyn S R and Ma B 1991 *Appl. Phys. Lett.* **58** 2165

[6] Ma P, Yang J, Gu H W, Chen L F, Li H and Liu Z X 1997 *Acta Phys. Sin.* **46** 198 (in Chinese)

[7] Goyal A, Norton D P, Christen D K, Specht E D, Paranthaman M, Kroeger D K, Budai J D, He Q, List F A, Feenstra R, Kerchner H R, Lee D F, Hatfield E, Martin P M, Mathis J and Park C 1996 *Applied Superconductivity* **4** 403

[8] Liu Z, Wang S F, Zhao S Q and Zhou Y L 2005 *Acta Phys. Sin.* **54** 5820 (in Chinese)

[9] Wang S F, Zhao S Q, Liu Z, Zhou Y L, Chen Z H, Lü H B, Jin K J, Cheng B L and Yang G Z 2006 *Chin. Phys.* **15** 444

[10] Barnes P N, Nekkanti R M, Haugan T J, Campbell T A, Yust N A and Evans J M 2004 *Supercond. Sci. Technol.* **17** 958

[11] Paranthaman M, Goyal A, List A, Specht E D, Lee D F, Martin P M, He Q, Christen D K, Norton D P, Budai J D and Kroeger D K 1997 *Physica* C **275** 266

[12] He Q, Christen D K, Budai J D, Specht E D, Lee D F, Goyal A, Norton D P, Paranthaman M, List F A and Kroeger D K 1997 *Physica* C **275** 155

[13] Yamada Y, Muroga T, Iwai H, Izumi T and Shiohara Y 2003 *Physica* C **392–396** 777

[14] Muroga T, Iwai H, Yamada Y, Izumi T, Shiohara Y, Iijima Y, Saito T, Kato T, Sugawara Y and Hirayama T 2003 *Physica* C **392-396** 796

[15] Yamada Y, Muroga T, Iwai H, Watanabe T, Miyata S and Shiohara Y 2004 *Supercond. Sci. Technol.* **17** S328